The Effects of Tenascin C Knockdown on Trabecular Meshwork Outflow Resistance

Kate E. Keller,[1] Janice A. Vranka,[1] Ramez I. Haddadin,[2] Min-Hyung Kang,[2] Dong-Jin Oh,[2] Douglas J. Rhee,[2] Yong-feng Yang,[1] Ying Ying Sun,[1] Mary J. Kelley,[1] and Ted S. Acott[1]

[1]Casey Eye Institute, Oregon Health & Science University, Portland, Oregon
[2]Massachusetts Eye and Ear Infirmary, Harvard Medical School, Boston, Massachusetts

Correspondence: Kate E. Keller, Casey Eye Institute, 3181 SW Sam Jackson Park Road, Portland, OR 97239; gregorka@ohsu.edu.

Submitted: January 7, 2013
Accepted: July 18, 2013

Citation: Keller KE, Vranka JA, Haddadin RI, et al. The effects of tenascin C knockdown on trabecular meshwork outflow resistance. *Invest Ophthalmol Vis Sci*. 2013;54:5613–5623. DOI:10.1167/iovs.13-11620

Purpose. Tenascin C (TNC) is a matricellular glycoprotein whose expression in adult tissue is indicative of tissue remodeling. The purpose of the current study was to determine the localization of TNC in trabecular meshwork (TM) tissue and to analyze the effects of TNC on intraocular pressure (IOP).

Methods. Human TM frontal sections were immunostained with anti-TNC and imaged by confocal microscopy. TNC mRNA and protein levels were quantitated in anterior segments perfused at physiological and elevated pressure. Short, hairpin RNA (shRNA) silencing lentivirus targeting full-length TNC (shTNC) was applied to anterior segment perfusion organ cultures. The IOPs and central corneal thickness (CCT) of wild-type, *TNC*$^{-/-}$, and tenascin X (*TNX*$^{-/-}$) knockout mice were measured.

Results. TNC was distributed in the juxtacanalicular (JCT) region of adult human TM, predominantly in the basement membrane underlying the inner wall of Schlemm's canal. Application of shTNC lentivirus to human and porcine anterior segments in perfusion culture did not significantly affect outflow rate. Although TNC was upregulated in response to pressure, there was no difference in outflow rate when shTNC-silenced anterior segments were subjected to elevated pressure. Furthermore, IOPs and CCTs were not significantly different between *TNC*$^{-/-}$ or *TNX*$^{-/-}$ and wild-type mice.

Conclusions. TNC does not appear to contribute directly to outflow resistance. However, TNC immunolocalization in the JCT of adult human eyes suggests that certain areas of the TM are being continuously remodeled with or without an IOP increase.

Keywords: tenascin C, trabecular meshwork, outflow resistance, extracellular matrix

Trabecular meshwork (TM) cells synthesize abundant extracellular matrix (ECM) that provides a permissive milieu through which TM cells can sense and respond to alterations in their environment.[1] Constituents of the ECM include collagens, elastic microfibrils, matricellular proteins, glycosaminoglycans (GAGs), and proteoglycans. The ECM of TM tissue appears to play a key role in establishing the resistance to aqueous humor outflow. Cellular modifications of the ECM lead to increased or reduced outflow in response to fluctuations in intraocular pressure (IOP).[2–10] TM cells sense elevated IOP, which is frequently associated with primary open-angle glaucoma, as mechanical stretching and/or distortion.[11] This generates a cascade of events that leads to the focal degradation of the existing ECM to allow greater aqueous outflow and synthesis of new ECM components to maintain the altered flow.[2,12] One ECM component that is highly upregulated in response to mechanical stretching of TM cells is the matricellular protein tenascin C.[13]

Tenascin C (TNC) is a large homohexameric glycoprotein that is expressed by TM cells.[14] It is one of four members of the tenascin family of genes, which includes tenascins X, R, and W.[15] In other tissues, tenascins function to modulate cellular responses, cellular growth, adhesion, migration, and apoptosis.[15–19] Although they are highly expressed during embryonic development, both TNC and tenascin X (TNX) have much lower and restricted expression in adult tissues.[15,18–20] However, TNC is re-expressed in areas of tissue undergoing active ECM remodeling.[19] TNC binds other extracellular and cell-surface proteins including fibronectin, versican, integrins, and syndecans.[20] It is a modular domain protein composed of multiple fibronectin type III (FnIII) repeats and epidermal growth factor (EGF) domains. Complex alternative splicing introduces up to nine extra FnIII repeats, which are termed A1, A2, A3, A4, B, C, D, ad1, and ad2, between constitutively expressed FnIII repeats 5 and 6.[17] Transcripts including all combinations of these alternate domains exist, but these are expressed in a tissue- and cell-specific manner.[17] In porcine TM cells, two major *TNC* splice forms were detected in approximately equal proportions: one containing no alternatively spliced domains and one containing FnIII repeat D.[21] Minor transcripts FnIII A1-B and FnIII B-D-6 were also detected, but transcripts containing FnIII A2, A3, A4, ad1, and ad2 were not detected by RT-PCR.[21] Moreover, *TNC* transcription was increased and inclusion of FnIII domain D increased over time when TM cells were subjected to mechanical stretch.[21] Since mechanical stretch likely triggers the homeostatic response, this suggests that one mechanism by which TM cells reduce IOP is by increasing transcription of *TNC*. This is consistent with its re-expression in areas of active remodeling in other tissues.

A specific role for certain matricellular proteins in IOP regulation is emerging. Genetic ablation of the matricellular proteins SPARC (secreted protein acidic and rich in cysteine) and thrombospondins-1 and -2 in the TM of mice lowers IOP.[22,23] However, targeted deletion of the matricellular proteins hevin and osteopontin does not change IOP in mice.[24,25] In light of these somewhat divergent roles of matricellular proteins in IOP regulation, we initiated this current study to elucidate the function of TNC in TM outflow resistance. TNC was immunolocalized in adult human TM tissue and compared to the distribution of fibrillin-1, an elastic fiber component that shows a similar pattern of distribution by immunoelectron microscopy.[26] In addition, the effect of RNA interference (RNAi) silencing was investigated in human and porcine perfused anterior segments with and without elevated pressure. Finally, IOPs and central corneal thicknesses (CCTs) were measured in TNC and TNX knockout mice.

Methods

Immunofluorescence and Microscopy

Immunostaining was performed on human anterior segments from donor eyes acquired from Lions Eye Bank of Oregon (Portland, OR). Use of donor eye tissue was approved by the Oregon Health & Science University Institutional Review Board, and experiments were conducted in accordance with the tenets of the Declaration of Helsinki for the use of human tissue. Anterior segments were perfused continuously either at constant pressure (8.8 mm Hg) to generate an average flow rate of 1 to 7 μL/min or under elevated pressure conditions at 16 mm Hg as described previously.[11] Fluorescent tracer (Qtracker 594- or 200-nm amine-modified, 594-labeled fluospheres; Invitrogen, Grand Island, NY) was added to the intake line for the final 15 minutes of perfusion in order to label segmental outflow patterns.[27]

At the end of perfusion, RNA was isolated from high ($n = 6$) and low ($n = 4$) flow regions of the human tissue (from four individuals, mean age 73.75 years ± 16.74), and TNC mRNA levels were quantitated by quantitative RT-PCR (qRT-PCR) as previously described.[27] For other anterior segments, tissue was immersion fixed in 4% paraformaldehyde, and frontal sections were cut with a double-edged razor blade perpendicular to the ocular surface, resulting in a section tangential to the corneoscleral limbus that bisects Schlemm's canal as described previously.[27–29] Three pairs of human eyes were used, and six different regions around the circumference of the eyes were analyzed. Tissues were blocked and incubated overnight at 4°C with a fibrillin-1 mouse monoclonal antibody (EMD Millipore, Billerica, MA) and a TNC rabbit polyclonal antibody (Ab19011; EMD Millipore). Primary antibodies were detected with Alexa-Fluor 488–conjugated anti-mouse and Alexa-Fluor 594– or 647–conjugated anti-rabbit secondary antibodies, respectively (Invitrogen). Sections were placed on glass slides and imaged by confocal microscopy. Image acquisition settings and number of sections stacked for each image were maintained between images. All images shown are from compressed z-stacks.

To assess colocalization, compressed confocal images ($n = 7$) showing typical TNC and fibrillin distributions were analyzed using Imaris Bitplane 3-D software (South Windsor, CT). Any pixel displaying fluorescence was brightened and filled in by the software since intensities of fluorescence are ignored. Each channel was then overlaid onto the original image, with colocalization results shown in yellow. The software then calculated Pearson's correlation coefficients for each combination of two color channels as indicated in Table 1. Based on the Pearson's values, the degree of colocalization was categorized as very strong (0.85–1.0), strong (0.49–0.84), moderate (0.1–0.48), weak (–0.26 to 0.09), or very weak (–1 to –0.27) according to a recently published grading system.[30]

Generation of TNC Short, Hairpin RNA (shRNA) Silencing Lentivirus

We generated shRNA vectors in order to silence the *TNC* gene as described previously.[27,29] Briefly, shRNAs were designed using the online BLOCK-iT RNAi designer (Invitrogen). The shRNA sequence targeting tenascin C (shTNC) was 5′-CACCGGGA GATCATCTTCCFFAATACGAATATTCCGGAAGATGATCTCCC-3′, which is located in the region encoding the second FnIII repeat and thus targets all isoforms of *TNC*. A shRNA negative control (shCtrl) was also included and has been previously characterized.[27] shRNA oligonucleotides were annealed and cloned into the pENTR/U6 vector using T4 ligase (Invitrogen). The correct sequence was confirmed by DNA sequencing, and the shRNA cassette was transferred into the pLenti6/BLOCK-iT-DEST vector (human immunodeficiency virus [HIV]-based lentiviral vector) by recombination using the Gateway LR clonase II enzyme (Invitrogen). To generate replication-incompetent lentivirus, 3 μg shTNC pLenti plasmid was cotransfected into the 293FT cell line with 9 μg ViraPower packaging mix (Invitrogen) using Lipofectamine 2000 (Invitrogen). Lentivirus-containing supernatants were harvested 72 hours posttransfection, and viral titers were determined as previously described.[27] Lentivirus was stored at –80°C until use.

Verification of Gene Knockdown by qRT-PCR and Western Blotting

Primary human trabecular meshwork (HTM) or porcine TM (PTM) cells were isolated from TM tissue and grown to confluence in Dulbecco's modified Eagle's medium (DMEM) containing 10% fetal bovine serum and 1% penicillin-streptomycin-fungizone.[31,32] Confluent TM cells were passaged and incubated with 10^6 plaque formation units (pfu) of shTNC or control shRNA lentivirus. After 4 days, total RNA was isolated using cells-to-cDNA lysis buffer (Invitrogen); cDNA was reverse transcribed from total RNA using Superscript III reverse transcriptase (Invitrogen). Quantitative RT-PCR was performed using primers in exons 3 and 6. Results were normalized to the 18S RNA housekeeping gene and expressed as a fold change relative to control shRNA-infected TM cells. Analysis of variance (ANOVA) was calculated, and $P < 0.05$ was considered statistically significant.

For analysis of TNC protein, TM cells were infected with shTNC and shCtrl lentivirus as above. After 3 days to allow silencing, medium was exchanged to serum-free DMEM for 72 hours, and protease inhibitor cocktail (Sigma-Aldrich, St. Louis, MO) was added. Proteins in the media or radio-immunoprecipitation assay (RIPA) cell lysates were separated on 7.5% SDS-polyacrylamide Ready gels (BioRad Laboratories, Hercules, CA) under reducing conditions. After transfer to nitrocellulose, Western blots were blocked with Odyssey blocking buffer (Li-Cor Biosciences, Lincoln, NE), probed with the TNC primary antibody, and detected using an IRDye700 goat anti-rabbit secondary antibody (Li-Cor Biosciences). Membranes were scanned on an Odyssey infrared imaging system with Odyssey 2.0 software.

Anterior Segment Perfusion Culture

Human eye tissue was obtained from cadavers, and anterior segments were placed into serum-free stationary organ culture for 5 to 7 days to allow cellular recovery postmortem.[33] The range and average age of the cadaver eyes was 62 to 92 and

Investigative Ophthalmology & Visual Science

Table 1. Pearson's Correlation Coefficients Calculated Between TNC and Fibrillin-1 Immunostaining, TNC and DAPI, and Fibrillin-1 and DAPI

Component 1	Color/Stain	Component 2	Color/Stain	Pearson's Correlation Coefficient
Fibrillin-1	Green/Alexa 488	Tenascin C	Red/Alexa 647	0.5071 ± 0.1328
Nuclei	Blue/DAPI	Fibrillin-1	Green/Alexa 488	−0.0891 ± 0.026
Nuclei	Blue/DAPI	Tenascin C	Red/Alexa 647	−0.0379 ± 0.0129

A positive value indicates colocalization, while a negative value indicates no significant overlap. The mean Pearson's coefficient ± standard deviation from seven images is reported.

82.5 ± 7.5 years, respectively. Porcine eyes were obtained from the local abattoir (Carlton Farms, Carlton, OR) and placed into perfusion culture within 4 hours of death. Human and porcine anterior segments were perfused with serum-free DMEM at constant pressure (8 mm Hg) until flow rates stabilized at an average flow rate of 1 to 7 μL/min for human and 2 to 8 μL/min for porcine.[34] Anterior segments that could not be stabilized at these flow rates were discarded. For experiments using increased pressure, the pressure head was doubled in height to provide approximately 16 mm Hg for the times indicated.[11] TNC silencing experiments were performed as described previously.[27,35,36] Briefly, lentivirus (10^8 pfu) was applied to the perfusion chambers by media exchange (indicated by time point 0), and outflow rates were measured for a further 5 to 7 days. For each eye, change in outflow rate was determined by normalizing to the average outflow rate prior to treatment. Data from individual eyes were then combined. The number of eyes used for each treatment is noted in the figure legend.

TNC mRNA and Protein Analysis at 2× Pressure

Human or pig eyes that had stabilized after perfusion at 1× pressure were perfused at 2× pressure for 24 hours (for mRNA analysis) or 48 hours (for protein analysis) as described previously.[37] Five human eye pairs (average age, 81.28 ± 2.03; age range, 74–91) were used for mRNA analysis. Following perfusion, the TM was dissected; RNA was extracted with Trizol (Invitrogen) and amplified using the MessageAmp II RNA amplification kit (Invitrogen).[37] The amplified RNA was reverse transcribed, and *TNC* mRNA levels were quantified using qRT-PCR as above and normalized for *GAPDH* gene levels. For Western immunoblot analysis, the TM was dissected from the tissue, placed in 100 μL RIPA buffer with proteinase inhibitor cocktail, and homogenized. Samples were centrifuged at 4000 revolutions per minute for 5 minutes to pellet insoluble debris. The supernatant was subject to Western immunoblot analysis as above, simultaneously probing with the TNC rabbit polyclonal antibody and a fibronectin mouse monoclonal antibody (BD Transduction Laboratories, San Jose, CA).

Measurement of IOP and CCT in TNC Knockout Mice

Adult $TNC^{-/-}$ knockout and wild-type mice were generated by Reinhard Fassler (Max Planck Institute of Biochemistry, Martinsried, Germany) and generously provided by Barry Stripp (Duke University, Durham, NC).[38] Tenascin X ($TNX^{-/-}$) knockout and wild-type mice were generously provided by James Bristow (University of California, San Francisco, CA).[39] All animal experiments were performed in compliance with the ARVO Statement for the Use of Animals in Ophthalmic and Vision Research, and animals were maintained according to the animal husbandry procedures described previously.[22–25] IOP was measured using a rebound tonometer as previously described.[22–25] Briefly, the mice were anesthetized by intraperitoneal injection (IP) of a mixture of ketamine and xylazine (100 and 9 mg/kg, respectively; Phoenix Pharmaceutica, St. Joseph, MO). A previously validated commercial rebound tonometer (TonoLab; Colonial Medical Supply, Franconia, NH) was fixed horizontally, with the tip of the probe positioned 2 to 3 mm from the eye, so that the probe contacted the eye perpendicularly at the central cornea. Verification of targeting was performed under direct visualization with ×5.5 magnification. A single measurement was accepted only if the device indicated that there was "no significant variability" (per the protocol manual; Colonial Medical Supply). Three sets of six measurements of IOP were taken in each eye.[40,41] To reduce the variability of measurements, the rebound tonometer was modified to include a pedal that activated the probe, obviating handling of the device. All measurements were taken between 4 and 7 minutes after IP injection because previous studies have shown this to be a period of stable IOP.[42,43] Right and left eye measurement sets were alternated, with the initial eye selected randomly. Daytime IOP measurements were taken between 1100 and 1500 hours.

Central corneal thickness may affect contact tonometry measurements by variable-force spring tonometers.[44] Therefore, CCTs were measured in $TNC^{-/-}$ and wild-type mice under anesthesia using optical coherence tomography (OCT; Stratus; Carl Zeiss Meditec, Inc., Dublin, CA) 1 week prior to IOP measurements. The process of locating the central corneal reflex was repeated three times by the same investigator, who was masked to the genetic status of the mouse, to produce three different images.[23] CCT was obtained using the OCT Stratus software (version 4.0.7) by measuring the peak-to-peak amplitude distance. IOP and CCT results were expressed as mean ± SD. Data from various experimental and control groups were compared using a Student's unpaired *t*-test. Differences were considered significant when $P < 0.05$.

Once CCTs and IOPs were measured, mice were further processed for histological staining.[22–25] For light microscopic studies, mice were killed with CO_2, and the eyes were enucleated. They were fixed with 10% formalin for 2 days and then dehydrated with 70% ethanol. The eyes were dehydrated in ascending concentrations of 95% ethanol for 2 hours. For methacrylate infiltration, the eyes were incubated with methacrylate (Technovit 7100; Heraeus Kulzer GmbH, Wehrheim, Germany) with Harder 1 (Technovit 7100; Heraeus Kulzer GmbH) overnight. For methacrylate embedding, the eyes were incubated with methacrylate (Technovit 7100; Heraeus Kulzer GmbH) with Harder 1 and 2 (Technovit 7100; Heraeus Kulzer GmbH) for 2 hours. Methacrylate sections were cut at 3 μm and were stained with toluidine blue. The slides were examined with an Olympus microscope (Olympus America, Center Valley, PA). Six eyes were examined for each genotype.

Gene Chip Microarray Analysis

Microarray analysis was essentially performed as described previously.[13] Primary PTM cells were serum starved for 48 hours prior to and during treatment with recombinant porcine TNFα or porcine IL-1α (both 10 ng/mL; R&D Systems, Minneapolis, MN) for 12, 24, or 48 hours. Control cells were

Investigative Ophthalmology & Visual Science

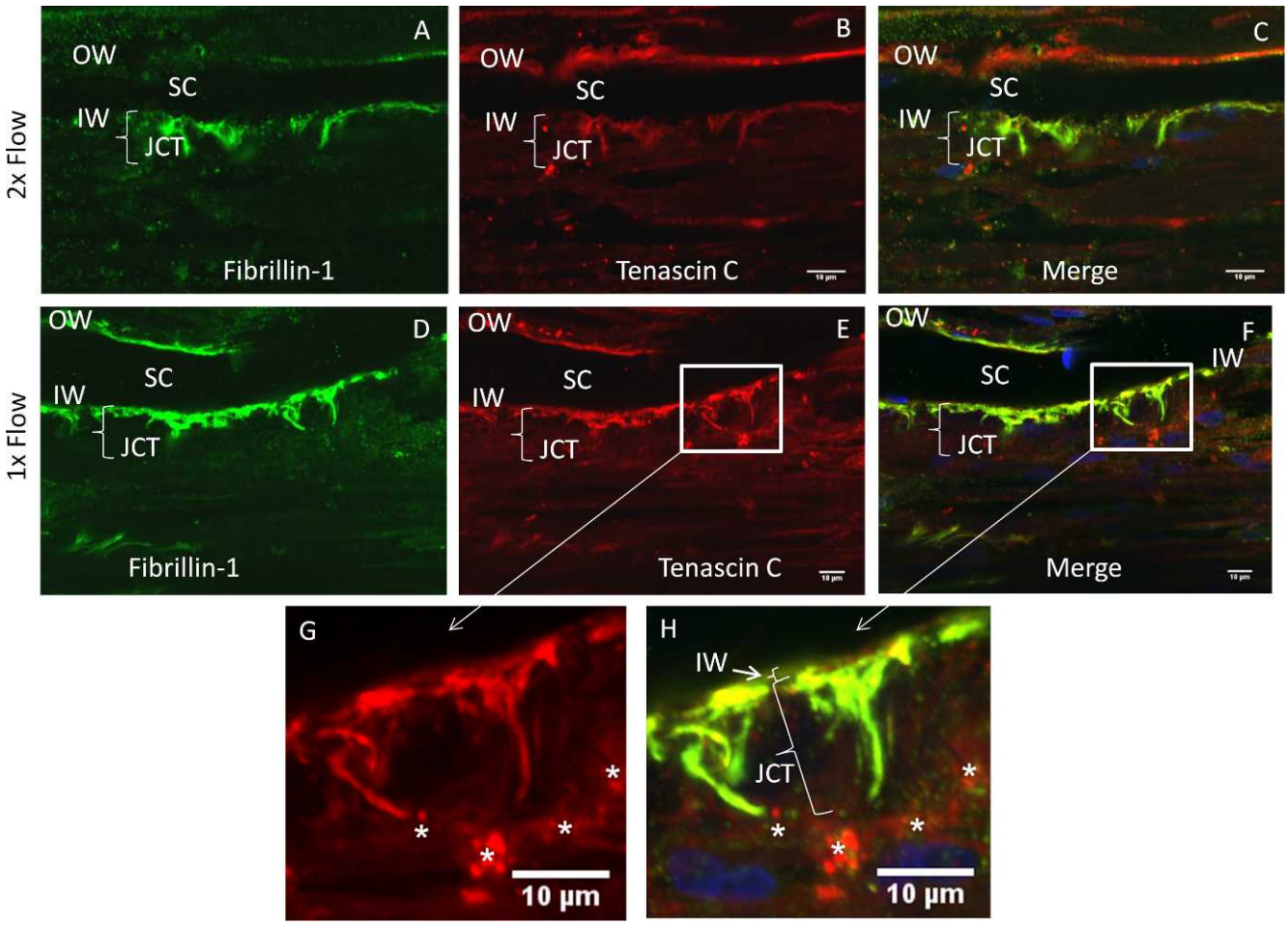

Figure 1. Immunofluorescence of TNC in trabecular meshwork tissue. Human anterior segments were cultured at physiological pressure (**D**–**H**) or at 2× pressure (**A**–**C**) for 24 hours. Tissue was fixed; frontal sections were cut and immunostained with TNC (*red*) and fibrillin-1 antibodies (*green*) (**A**–**H**). Single channels are shown for each protein, and a merged image with DAPI-stained nuclei is also shown (**C**, **F**, **H**). Higher-magnification images of boxed regions are also shown (**G**, **H**). Note that the bright spherical dots in the red channel may be Qdots (*white stars*), since these images were from tissue labeled for low segmental outflow. Size of JCT parentheses marker is 14 µm. OW, outer wall; IW, inner wall; SC, Schlemm's canal; JCT, juxtacanalicular region. *Scale bars*: 10 µm.

left untreated. Media were collected, treated with proteinase inhibitor cocktail (Sigma-Aldrich), and stored at –80°C for later Western blot analysis. Total RNA from TM cells was isolated using Trizol reagent (Invitrogen) according to the manufacturer's instructions. Three complete and totally independent experiments were conducted at all three time points using different cells, and samples were processed separately to give three independent biological samples. RNA samples (9 µg) from each time point (12, 24, or 48 hours) were processed at the Oregon Health & Science University Spotted Microarray Core (SMC) (Oregon Health & Science University, Portland, OR). Two human cDNA microarrays were printed per slide, giving each slide a maximum total of 16,896 spots (8448 different cDNAs). Hybridized arrays were scanned on a ScanArray 4000 XL (PerkinElmer, Boston, MA), and data were analyzed using ImaGene (BioDiscovery, Marina del Rey, CA). The resultant data were then preprocessed (normalized, centralized, and standardized) using intensity-based local regression implemented by the R language package from BioConductor (provided in the public domain primarily by the Fred Hutchinson Cancer Research Center, Seattle, WA). The treatment and control data were then corrected for background and normalized via Lowess[45] using GeneSpring software (Agilent/Silicon Genetics; Redwood City, CA) and statistically analyzed using SAM (Significance Analysis of Microarrays) software, as described previously.[13]

To verify mRNA data, Western immunoblots were performed with rabbit anti-SPARC (AB1858; EMD Millipore) on media samples collected from TM cells subjected to mechanical stretch for 48 or 72 hours. Briefly, TM cells were plated on membrane inserts in six-well culture dishes, and these membranes were mechanically stretched over a glass bead as described previously.[11] Gel bands were quantitated using FIJI software (in the public domain at http://fiji.sc/wiki/index.php/Fiji) following background correction. Average pixel intensity was calculated for control and stretched samples and presented as a percentage of the control at each time point. Significance was determined using a paired Student's *t*-test where $P < 0.05$ was considered significant.

Results

Tenascin C Localization in the TM

TNC protein was immunolocalized in frontal sections of adult human TM (Figs. 1B, 1E, 1G). In human TM tissue, TNC was most noticeable in the juxtacanalicular (JCT) region of the TM, particularly in the basement membrane region underlying the

Investigative Ophthalmology & Visual Science

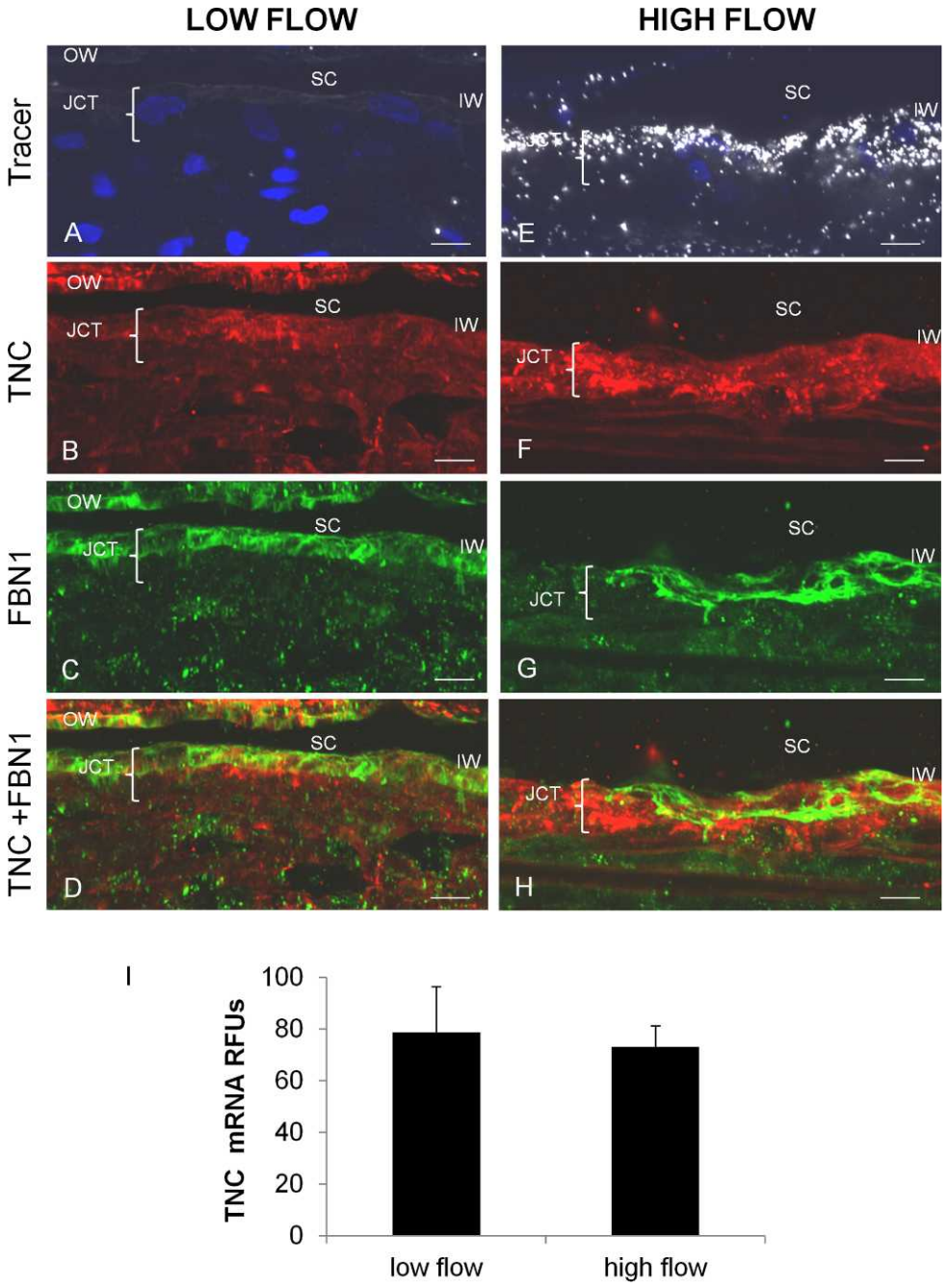

Figure 2. TNC immunostaining and mRNA levels in high and low outflow regions. Human anterior segments were labeled with 594-nm-labeled fluospheres ([**A**, **E**], *white*). The distribution of TNC ([**B**, **F**], *red*) and fibrillin-1 ([**C**, **G**], *green*) immunostaining and their colocalization (**D**, **H**) were assessed. OW, outer wall; IW, inner wall; SC, Schlemm's canal; JCT, juxtacanalicular region. *Scale bars*: 10 μm. (**I**) *TNC* mRNA levels (relative fluorescent units) in high and low outflow regions by quantitative RT-PCR normalized for GAPDH mRNA levels. Low flow, $n = 4$; high flow, $n = 6$. No significant difference was found.

inner wall of Schlemm's canal. However, little inner wall (IW) staining was observed (see position of TNC immunostaining in comparison to IW nucleus in Figure 1F and at the designated inner wall in Figure 1H [arrow]). TNC was also detected in the corneoscleral meshwork and outer wall of Schlemm's canal. Fibrillin-1, a component of microfibrils, was also localized (Figs. 1A, 1D), and some fibrillin immunostaining was colocalized with TNC (Figs. 1C, 1F, 1H).

TNC immunostaining in low and high outflow regions was analyzed (Fig. 2). The level of fluorescent tracer indicated areas of low and high outflow (Figs. 2A, 2E). In immunofluorescence images, there appeared to be more intense TNC immunostaining in the high flow region (Fig. 2F) than the low flow region (Fig. 2B). However, when multiple different areas of eyes from at least three individuals were analyzed, variability was apparent and there was no consistent pattern in the intensity of TNC immunostaining between high and low regions. No significant difference in TNC mRNA levels in high and low flow regions was detected upon qRT-PCR analysis of TM from four individuals (Fig. 2I).

Imaris Bitplane software was used to evaluate immunostaining colocalization. Pearson's correlation coefficients were

Investigative Ophthalmology & Visual Science

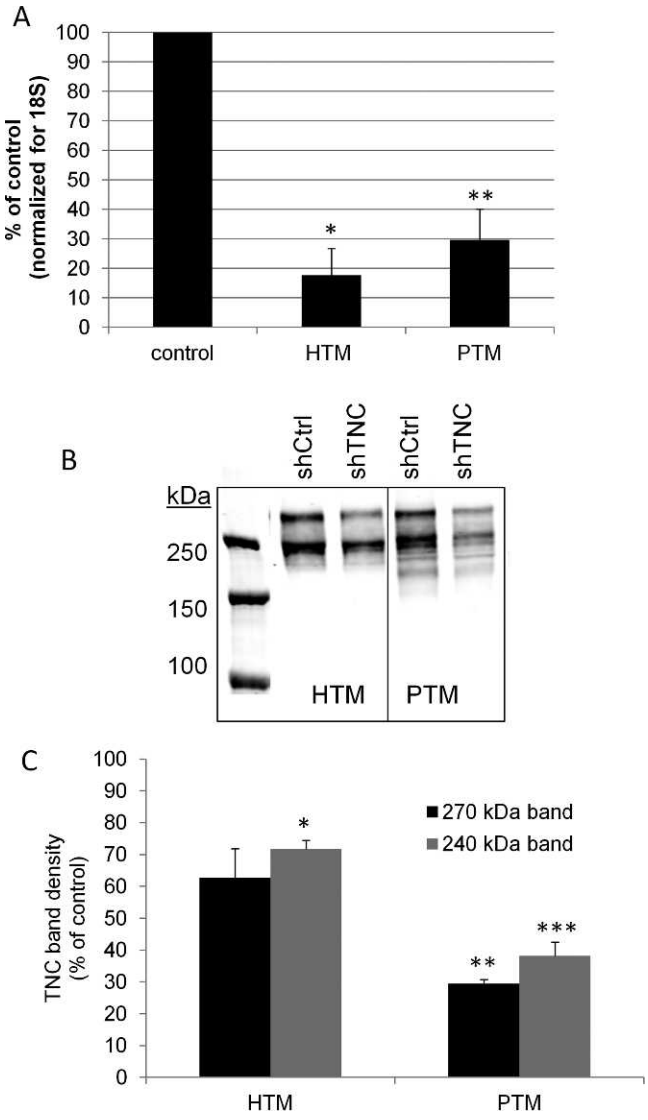

Figure 3. Generation of silencing lentivirus targeting TNC. (**A**) Quantitative RT-PCR to measure *TNC* mRNA levels in shTNC-infected human TM (HTM) and porcine TM (PTM) cells. $^{*}P = 0.0001$ and $^{**}P = 0.001$ by ANOVA; $n = 4$. (**B**) Western immunoblot showing knockdown of TNC in the media from control (shCtrl) and shTNC-infected HTM and PTM cells. Two bands at approximately 270 kDa and 240 kDa were detected. (**C**) Densitometry quantitation of the two bands showed a significant decrease in protein levels in shTNC-infected TM cells compared to control cells. $^{*}P = 0.009$; $^{**}P = 0.0001$; $^{***}P = 0.005$ by ANOVA; $n = 2$.

calculated from multiple images showing typical overlap distributions (Table 1). The Pearson's coefficient is a quantitative measurement used to estimate the degree of overlap between fluorescence signals obtained in two channels.[30,46] Similarity between shapes is taken into consideration, but differences in intensities of signals are ignored. Pearson's coefficient ranges between 1.0 and −1.0, where 1.0 indicates complete colocalization of two structures, 0 indicates no significant correlation, and −1.0 indicates no correlation.[30] The Pearson's coefficient between TNC and fibrillin-1 immunostaining (0.5071 ± 0.1328) indicates strong, but not complete, colocalization of these two proteins (Table 1). The Pearson's coefficients of TNC- and 4′,6-diamidino-2-phenylindole (DAPI)-stained nuclei, or fibrillin-1 and DAPI, were also calculated to act as negative controls. These were –0.0379 ± 0.0129 and –0.0891 ± 0.0261, respectively, which signifies no significant overlap of staining. The Pearson's coefficients between TNC and fibrillin-1 were very similar in regions of high, medium, and low flow with means ranging from 0.42 to 0.51.

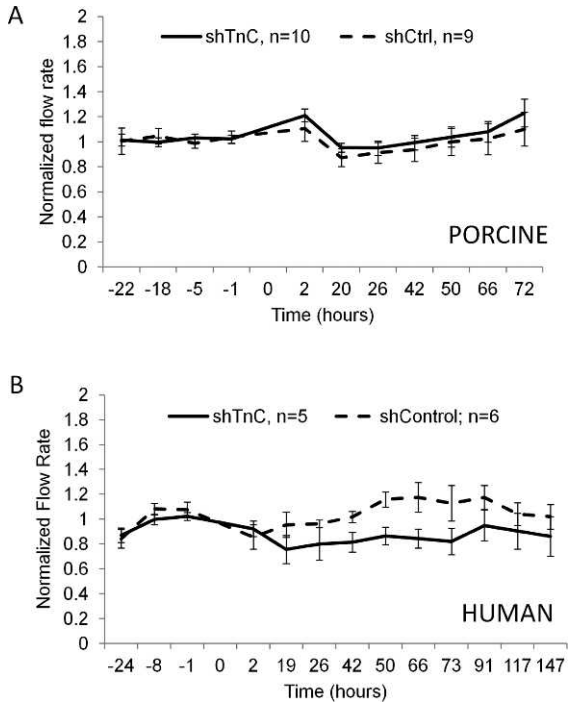

Figure 4. Porcine eyes (**A**) and human eyes (**B**) perfused at physiological pressure. Lentivirus was applied at time point 0, and outflow rates were monitored for a further 72 (porcine) or 147 (human) hours. No significant difference was observed between control and shTNC-infected anterior segments. *Error bars* signify the standard error of the mean. The number of eyes is indicated in the legend.

Effects of Tenascin C on Outflow

Next, we assessed whether reduced levels of TNC affect outflow. We generated tenascin C (shTNC) and control silencing lentivirus. To test the efficacy of *TNC* gene knockdown, quantitative RT-PCR was performed on human and porcine TM cells infected for 96 hours with TNC silencing lentivirus. Compared to shControl-infected TM cells, the shTNC lentivirus was found to knock down approximately 80% of human transcripts and 70% of porcine transcripts (Fig. 3A). To assess TNC protein knockdown, Western immunoblots were performed and densitometry was used to quantitate the immunoreactive bands (Fig. 3B). Two bands were detected: one at approximately 240 kDa, which is consistent with a full-length chain without inclusion of alternatively spliced domains, and an upper band, which likely represents an alternatively spliced isoform of TNC containing additional FnIII repeat(s).[21] The immunoblots shown are from media samples, but RIPA cell lysates were also analyzed with similar results. Densitometry of Western immunoblots showed that application of shTNC for 6 days, which allows for infection and turnover of established TNC, knocked down approximately 40% of TNC protein in HTM cells and 70% in PTM cells (Fig. 3C). To test the effect of *TNC* gene knockdown on outflow, lentivirus was applied to human and porcine anterior segments in perfusion culture. As shown in Figure 4, knockdown of the *TNC* gene did not significantly alter outflow rates in porcine (Fig. 4A) or human (Fig. 4B) anterior segments compared to

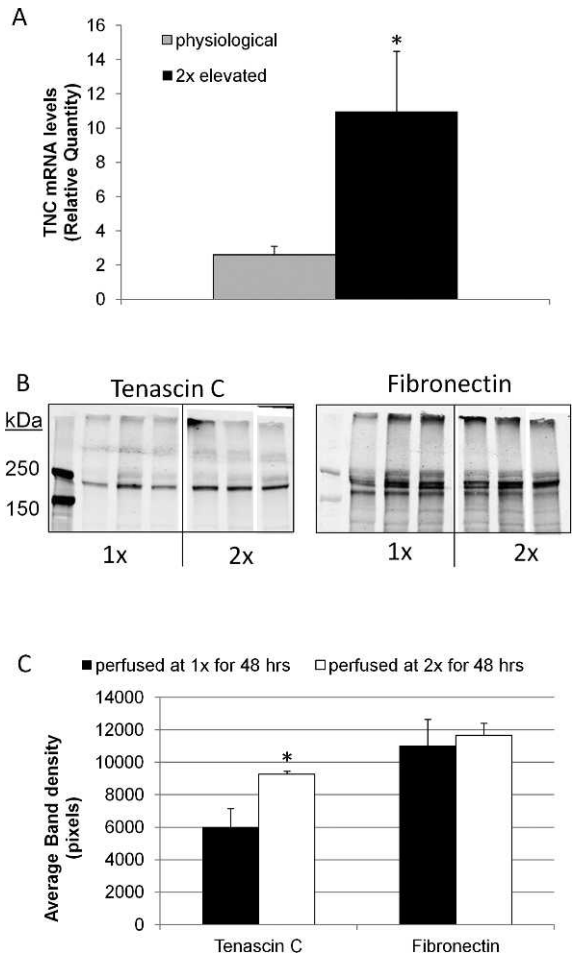

Figure 5. *TNC* mRNA and protein levels in response to elevated pressure. (**A**) Human eyes were perfused at physiological or 2× elevated pressure for 24 hours. RNA was isolated from TM tissue, and the *TNC* mRNA levels were quantitated using qRT-PCR and normalized for GAPDH mRNA levels. *Error bars* signify the standard error of the mean. $^*P = 0.047$ by a Student's *t*-test, $n = 5$. (**B**) Western immunoblots of tenascin C and fibronectin in RIPA extracts of TM tissue dissected from anterior segments perfused at physiological or 2× pressure for 48 hours. The immunoblots were simultaneously probed with both antibodies. Three replicates are shown for each treatment. (**C**) Quantitation of tenascin C and fibronectin bands by densitometry. *Error bars* signify the standard error of the mean. $^*P = 0.047$; $n = 3$.

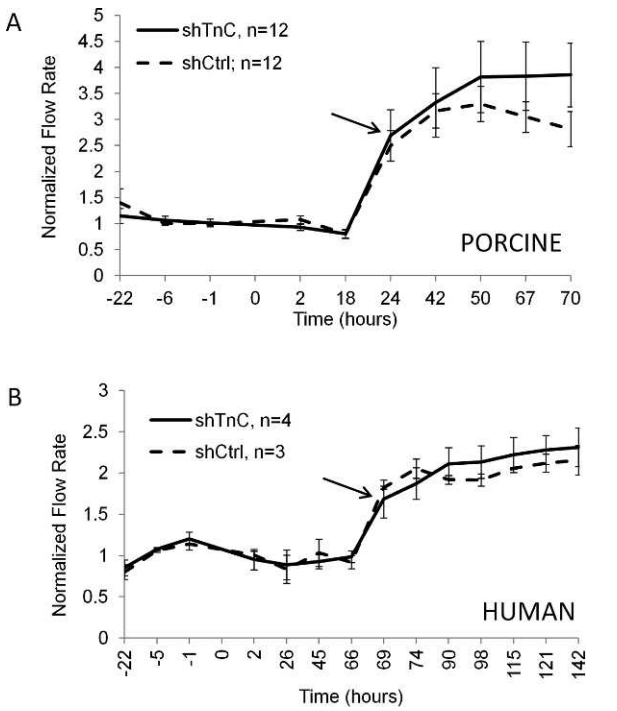

Figure 6. Porcine eyes (**A**) and human eyes (**B**) perfused at 2× pressure. shTenascin C (shTNC) silencing lentivirus and shControl (shCtrl) lentivirus were applied to anterior segments at time point 0, and the pressure head was doubled at 19 hours for porcine eyes or 67 hours for human eyes. Outflow rates were measured for a further 50 and 75 hours, respectively. No significant difference was observed between control and shTNC-infected anterior segments. *Error bars* signify the standard error of the mean. The number of eyes is indicated in the legend. *Arrows* mark initiation of gradual IOP homeostatic resistance adjustment.

control lentivirus. Actual outflow rate data can be found in Supplementary Tables S1 and S2.

Previously, we reported that *TNC* mRNA and protein levels were increased in response to mechanical stretching of cultured TM cells.[13] In order to evaluate the response of TNC in human anterior segments subjected to increased (2×) pressure, we performed quantitative RT-PCR. *TNC* mRNA levels were significantly increased approximately 2-fold following a pressure increase of 8 mm Hg for 24 hours in human anterior segments compared to contralateral control eyes, which were maintained at physiological (1×) pressure (Fig. 5A). Western immunoblotting was also performed on TNC and fibronectin protein extracted from the TM of pig eyes perfused at 2× pressure for 48 hours (Fig. 5B). Although there was some variability, especially at 1× pressure, densitometry showed an approximately 1.53-fold increase in TNC protein ($n = 3$; $P = 0.047$), while fibronectin was not significantly increased (Fig. 5C).

Since TNC is upregulated in response to pressure, we then asked whether subjecting shTNC-infected eyes to increased pressure would elicit an altered outflow response compared to control-infected eyes. After stabilizing the flow rates for 22 hours, shTNC or shCtrl lentivirus was applied to human and porcine anterior segments in perfusion culture; and after 24 hours (porcine) or 69 hours (human), the pressure head was doubled. Outflow was monitored for a further 46 (porcine) or 73 hours (human). A normal IOP homeostatic response, shown by gradually increasing flow rates after the initial approximately 2× flow increase (beginning at the arrow), was observed following the pressure elevation in both porcine and human anterior segments in shCtrl-infected eyes (Fig. 6). Infection with shTNC silencing lentivirus did not appreciably change the homeostatic response in human eyes (Fig. 6B) and only slightly changed it in porcine eyes (Fig. 6A). The difference between control and shTNC-infected outflow curves in porcine eyes was not significant.

Effects of Tenascin C in Knockout Mice

IOP was measured in *TNC* knockout mice (Table 2). Wild-type mice had an average IOP of 17.8 mm Hg ± 1.9, while homozygous $TNC^{-/-}$ littermates had an average IOP of 18.1 mm Hg ± 1.5, which was not significantly different. Central corneal thickness was also similar in knockout mice (102.4 ± 4.4 μm in wild-type and 102.3 ± 4.5 μm in $TNC^{-/-}$ homozygotes). Moreover, no obvious histological changes were seen in toluidine blue–stained sections of mouse eyes (Figs. 7A, 7B). Tenascin X is another matricellular protein that

Table 2. Average IOP and CCT Measurements of TNC Wild-Type and Homozygous Null Mice

Tenascin C	IOP	CCT	SD	*N*	*P* Value
Wild type ($^{+/+}$)	17.8		1.9	60	0.290
Knockout ($^{-/-}$)	18.1		1.5	60	
Wild type ($^{+/+}$)		102.4	4.4	69	0.856
Knockout ($^{-/-}$)		102.3	4.5	74	

P values were calculated from Student's *t*-tests (n = eyes). Data show the mean ± standard deviation (SD).

is closely related to TNC.[15] Therefore, IOPs and CCTs were also measured in *TNX* knockout mice. The IOPs of $TNX^{+/+}$ and $^{-/-}$ were 17.8 ± 1.8 mm Hg and 17.5 ± 1.5 mm Hg, respectively ($P = 0.201$; $n = 60$ and 74, respectively). The CCTs of $TNX^{+/+}$ and $^{-/-}$ were 103.5 ± 4.4 μm and 102.8 ± 4.8 μm, respectively ($P = 0.282$; $n = 79$ and 89, respectively). Again, these results show no significant difference between *TNX* homozygous mice and wild-type littermates. In addition, no histological changes were noted in toluidine blue–stained sections (Figs. 7C, 7D).

Effects of Various Treatments That Increase Outflow on Tenascin C and SPARC Expression

SPARC is a matricellular protein that is expressed in TM and, in contrast to TNC, its genetic ablation lowers IOP in mice.[14,23,47] To further explore the differential regulation of matricellular proteins in TM cells and their conflicting roles in IOP regulation, we investigated the temporal response of *TNC* and *SPARC* mRNA to various stimulations that increase outflow facility (Bradley JM, et al. *IOVS* 2006;47:ARVO E-Abstract 1865). *TNC* and *SPARC* mRNA levels were measured by microarray in PTM cells subjected to mechanical stretch, TNFα, and IL-1α for 12, 24, and 48 hours (Table 3). The mechanical stretch data were published previously,[13] but are included here for brevity and comparison. In general, *TNC* mRNA levels showed the greatest changes at the earlier time points (12 and 24 hours) with all three treatments, and the responses were relatively diminished by 48 hours. Conversely, alterations of SPARC mRNA levels were mild at 12 hours, but differences became more evident over time, and changes were most apparent at the 48-hour time point for all three treatments. Western immunoblots of TM cells in response to mechanical stretch at 48 and 72 hours confirmed the upregulation of SPARC protein (Fig. 8).

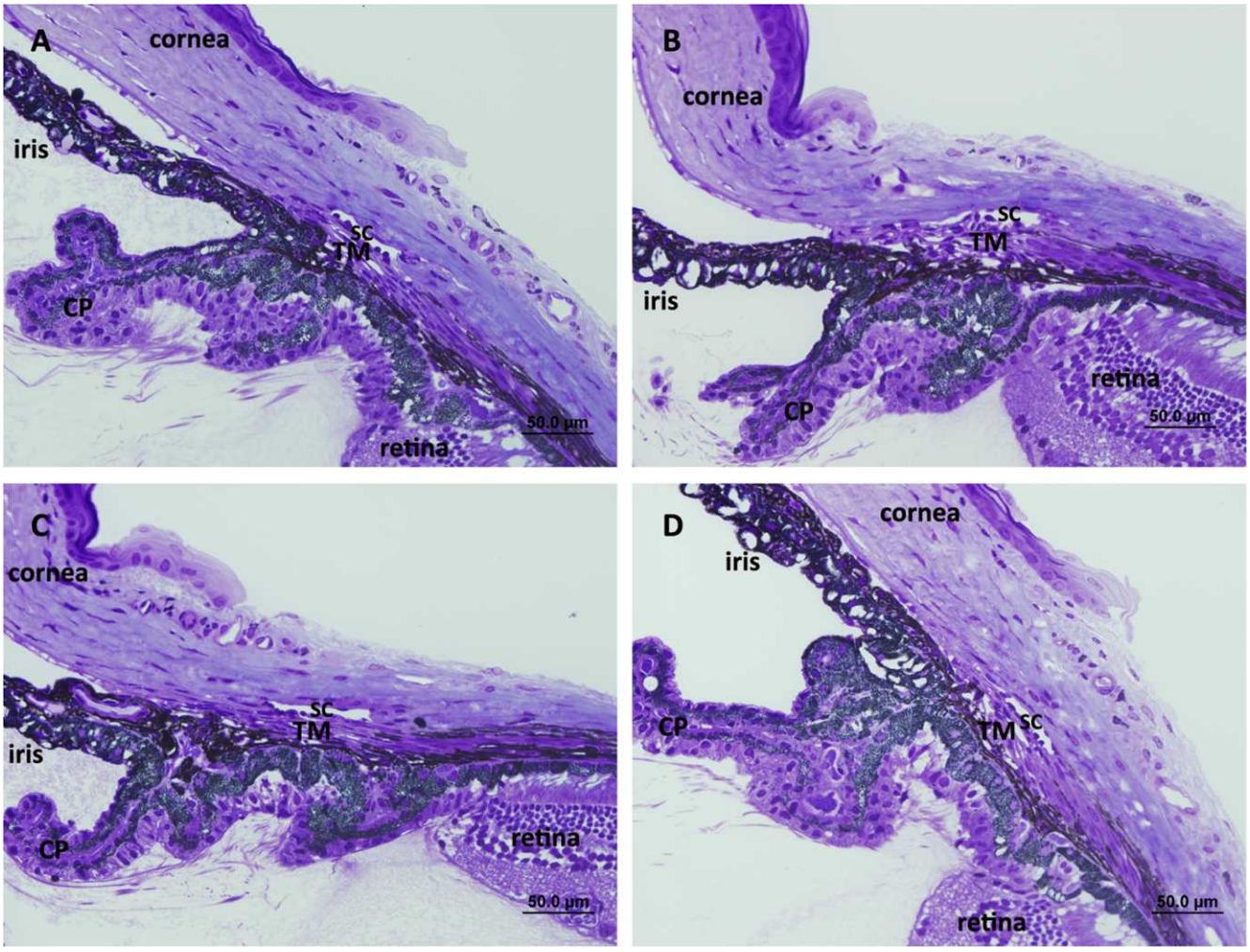

Figure 7. Light microscopic images of iridocorneal angles of (**A**) *TNC* wild-type, (**B**) *TNC*-null, (**C**) *TNX* wild-type, and (**D**) *TNX*-null mice. Schlemm's canal (SC), trabecular meshwork (TM) beams and cellularity, uveoscleral outflow pathway, and ciliary body location appeared grossly indistinguishable between *TNC* wild-type and *TNC*-null and between *TNX* wild-type and *TNX*-null mice, respectively. CP, ciliary processes. *Scale bar*: 50 μm.

Table 3. *TNC* and *SPARC* mRNA Levels by Microarray in Response to Mechanical Stretch, TNFα, and IL-1α Treatment for 12, 24, and 48 Hours

	12 h	24 h	48 h
Tenascin C			
Mechanical stretch	2.59	1.924	1.5
TNFα	3.67	4.22	NS
IL-1α	3.69	2.96	2.61
SPARC			
Mechanical stretch	1.68	1.964	2.417
TNFα	NS	1.57	1.53
IL-1α	NS	NS	0.48

Numbers represent fold change from untreated control. Mechanical stretch values were previously published.[13] NS, no significant change.

Discussion

Previous electron microscopy immunolabeling studies showed that TNC was a component of the core and outer sheath material of microfibrils of the elastic fiber cribriform plexus in human eyes.[26] Using confocal microscopy and immunofluorescence of frontal sections, in this study we show that TNC is predominantly distributed in the JCT ECM, in the basement membrane underlying the IW of Schlemm's canal. We observed more TNC immunostaining in the deeper JCT than did previous studies, probably due to method differences.[26] In TNC and TNX knockout mice, we could detect no overt changes in the overall structure of the TM upon histological analysis compared to their wild-type counterparts. However, this does not preclude the possibility that ultrastructural changes could have occurred, since we did not perform electron microscopy.

In addition to tenascin C, other ECM proteins have been immunolocalized to the JCT including versican, fibronectin, hyaluronan (as detected with hyaluronan-binding protein), and the elastic fiber components fibrillin-1 and microfibrillar-associated protein-1/2.[27,29,48] This suggests that the deepest portion of the JCT, just beneath the IW endothelium, may have specialized functions. Previous studies that manipulated protein or GAG levels in human anterior segment perfusion cultures suggest that versican, fibronectin, and hyaluronan have roles in outflow resistance.[27,34,36,49,50] Congruence of multiple ECM proteins in this region may indicate a role in the outflow resistance.

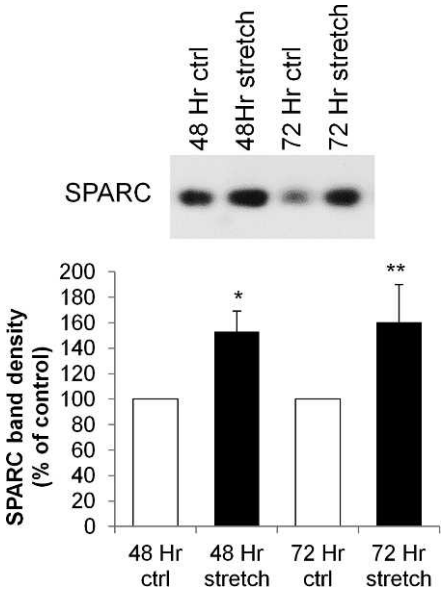

Figure 8. Representative Western immunoblots of SPARC in response to mechanical stretch of porcine TM cells for 48 and 72 hours. Stretch values represent percentage of nonstretched control cells by densitometry. $^{*}P = 0.0178$ and $^{**}P = 0.0404$ by a paired Student's *t*-test, $n = 4$.

The results of this study suggest that TNC does not directly contribute to outflow resistance, which hints at a more subtle function for TNC. In wound healing, TNC re-expression correlates with zones of excessive matrix deposition and delay of wound closure until an appropriate matrix is synthesized and rebuilt.[51,52] Midwood et al. also suggest that TNC may define the boundaries of the wound bed. In analogy, we speculate that TNC in aqueous outflow pathways may function to delineate the outflow and orchestrate deposition and organization of newly synthesized ECM in order to facilitate aqueous outflow through the JCT to Schlemm's canal.

Mechanical stretching of TM cells, which appears to trigger the IOP homeostatic response, was found to significantly increase *TNC* mRNA expression.[13] Consistent with this, we found that *TNC* mRNA and protein were also upregulated in perfused anterior segments in response to increased pressure. Since increased pressure triggers ECM turnover, upregulation of TNC is consistent with re-expression of TNC during active remodeling of tissues.[18,19] Due to this rapid upregulation, we might expect that outflow rate in TNC-silenced eyes would be accelerated or delayed or the magnitude of response altered after increasing pressure. However, no significant difference was found in either TNC-silenced porcine or human anterior segments following application of pressure. This was somewhat surprising since TNC can modulate ECM protein–protein interactions and cell adhesion.[53,54] There was a modest but not significant difference noted between TNC-silenced and control-infected porcine eyes subjected to increased pressure. Given that matricellular proteins do not generally serve structural roles in the ECM,[55] the small difference in outflow in response to pressure in porcine eyes could represent modulation of cell–matrix interactions in order to facilitate changes in outflow resistance. Unfortunately, longer experiments using porcine eyes cannot be performed, since the anterior segments deteriorate significantly if cultured for more than 5 days (Keller KE, Bradley JM, Acott TS, unpublished observations, 2008).

Contrary to the results found for TNC, knockout of other matricellular proteins including SPARC and thrombospondins-1 and -2 lowers IOP in mouse eyes.[22,23] Previously, our laboratory found that *TNC* and *SPARC* mRNA expression were both upregulated in response to mechanical stretch of TM cells, but their temporal response was different: *TNC* mRNA showed the highest upregulation at 12 hours following initiation of mechanical stretch, but the response tapered off at 24 and 48 hours of treatment.[13] Conversely, *SPARC* mRNA was modestly upregulated at 12 hours after stretch, but levels were further augmented at 24 and 48 hours.[13] In this study, similar temporal responses for *TNC* and *SPARC* mRNA were detected in response to TNFα and IL-1α treatment, both of which increase outflow rate in perfusion culture (Bradley JM, et al. *IOVS* 2006;47:ARVO E-Abstract 1865).[56] Differences in the temporal responses may reflect different functional roles for these two matricellular proteins during the remodeling process. Extracellular matrix remodeling appears to consist of two phases: degradation of existing ECM and synthesis of replacement components to maintain the modified resistance.[1,2] Since *TNC* is upregulated at early time points, we speculate that TNC might have an important biological function in the first phase of degradation of existing ECM. Alternatively, TNC could signal to the cell or relate signals back to the ECM via its interaction with integrins.[20] Whatever the function of TNC, this does not apparently directly impact

outflow resistance. In contrast, because SPARC has higher mRNA expression at 48 hours, SPARC may perform essential roles in the later phases of remodeling, when replacement ECM is synthesized. SPARC binds collagens and regulates basal lamina assembly.[57] Without SPARC to perform this crucial ECM assembly role, it is possible that the modified resistance cannot be maintained, which leads to the observed IOP reduction in knockout mice.[23] In this regard, type IV collagen assembly may be particularly susceptible to SPARC concentration since overexpression of SPARC by adenoviral delivery to perfused human eyes increased both outflow facility and collagen type IV immunostaining.[58]

In conclusion, while TNC does not appear to be an essential component of the outflow resistance, its expression and localization in adult TM tissue may denote areas of active remodeling. The apparent high expression levels of TNC in adult TM tissue points to a subtle yet important function in the ECM, both in eyes at physiological pressure and as TM cells homeostatically respond to elevated pressure.

Acknowledgments

The authors thank Ruth Phinney (Lions Eye Bank, Portland, Oregon) for facilitating the procurement of human donor eyes.

Supported by NIH Grants EY019643 (KEK), EY003279, EY008247, EY010572 (TSA), EY019654 (DJR); the Fight for Sight Summer Research Program (RIH); the Northwest Health Foundation (MJK); and an unrestricted grant to the Casey Eye Institute from Research to Prevent Blindness, New York, New York.

Disclosure: **K.E. Keller**, None; **J.A. Vranka**, None; **R.I. Haddadin**, None; **M.-H. Kang**, None; **D.-J. Oh**, None; **D.J. Rhee**, None; **Y.-F. Yang**, None; **Y.Y. Sun**, None; **M.J. Kelley**, None; **T.S. Acott**, None

References

1. Acott TS, Kelley MJ. Extracellular matrix in the trabecular meshwork. *Exp Eye Res*. 2008;86:543–561.
2. Keller KE, Aga M, Bradley JM, Kelley MJ, Acott TS. Extracellular matrix turnover and outflow resistance. *Exp Eye Res*. 2009;88:676–682.
3. Tamm ER. The trabecular meshwork outflow pathways: structural and functional aspects. *Exp Eye Res*. 2009;88:648–655.
4. Fuchshofer R, Tamm ER. Modulation of extracellular matrix turnover in the trabecular meshwork. *Exp Eye Res*. 2009;88:683–688.
5. Tane N, Dhar S, Roy S, Pinheiro A, Ohira A. Effect of excess synthesis of extracellular matrix components by trabecular meshwork cells: possible consequence on aqueous outflow. *Exp Eye Res*. 2007;84:832–842.
6. Fleenor DL, Shepard AR, Hellberg PE, Jacobson N, Pang IH, Clark AF. TGFbeta2-induced changes in human trabecular meshwork: implications for intraocular pressure. *Invest Ophthalmol Vis Sci*. 2006;47:226–234.
7. Goel M, Picciani RG, Lee RK, Bhattacharya SK. Aqueous humor dynamics: a review. *Open Ophthalmol J*. 2010;4:52–59.
8. Pattabiraman PP, Rao PV. Mechanistic basis of Rho GTPase-induced extracellular matrix synthesis in trabecular meshwork cells. *Am J Physiol Cell Physiol*. 2010;298:C749–C763.
9. Stamer WD, Acott TS. Current understanding of conventional outflow dysfunction in glaucoma. *Curr Opin Ophthalmol*. 2012;23:135–143.
10. Acott TS, Keller KE, Kelley MJ. Role of proteoglycans in the trabecular meshwork. In: Dartt DA, Besharse JC, Dana R, eds. *Encyclopedia of the Eye*. San Diego: Elsevier; 2010:170–178.
11. Bradley JM, Kelley MJ, Zhu X, Anderssohn AM, Alexander JP, Acott TS. Effects of mechanical stretching on trabecular matrix metalloproteinases. *Invest Ophthalmol Vis Sci*. 2001;42:1505–1513.
12. Aga M, Bradley JM, Keller KE, Kelley MJ, Acott TS. Specialized podosome- or invadopodia-like structures (PILS) for focal trabecular meshwork extracellular matrix turnover. *Invest Ophthalmol Vis Sci*. 2008;49:5353–5365.
13. Vittal V, Rose A, Gregory KE, Kelley MJ, Acott TS. Changes in gene expression by trabecular meshwork cells in response to mechanical stretching. *Invest Ophthalmol Vis Sci*. 2005;46:2857–2868.
14. Rhee DJ, Haddadin RI, Kang MH, Oh DJ. Matricellular proteins in the trabecular meshwork. *Exp Eye Res*. 2009;88:694–703.
15. Hsia HC, Schwarzbauer JE. Meet the tenascins: multifunctional and mysterious. *J Biol Chem*. 2005;280:26641–26644.
16. Chiquet-Ehrismann R. Tenascins. *Int J Biochem Cell Biol*. 2004;36:986–990.
17. Jones FS, Jones PL. The tenascin family of ECM glycoproteins: structure, function, and regulation during embryonic development and tissue remodeling. *Dev Dyn*. 2000;218:235–259.
18. Jones PL, Jones FS. Tenascin-C in development and disease: gene regulation and cell function. *Matrix Biol*. 2000;19:581–596.
19. Midwood KS, Hussenet T, Langlois B, Orend G. Advances in tenascin-C biology. *Cell Mol Life Sci*. 2011;68:3175–3199.
20. Chiquet-Ehrismann R, Chiquet M. Tenascins: regulation and putative functions during pathological stress. *J Pathol*. 2003;200:488–499.
21. Keller KE, Kelley MJ, Acott TS. Extracellular matrix gene alternative splicing by trabecular meshwork cells in response to mechanical stretching. *Invest Ophthalmol Vis Sci*. 2007;48:1164–1172.
22. Haddadin RI, Oh DJ, Kang MH, et al. Thrombospondin-1 (TSP1)-null and TSP2-null mice exhibit lower intraocular pressures. *Invest Ophthalmol Vis Sci*. 2012;53:6708–6717.
23. Haddadin RI, Oh DJ, Kang MH, et al. SPARC-null mice exhibit lower intraocular pressures. *Invest Ophthalmol Vis Sci*. 2009;50:3771–3777.
24. Chowdhury UR, Jea SY, Oh DJ, Rhee DJ, Fautsch MP. Expression profile of the matricellular protein osteopontin in primary open-angle glaucoma and the normal human eye. *Invest Ophthalmol Vis Sci*. 2011;52:6443–6451.
25. Kang MH, Oh DJ, Rhee DJ. Effect of hevin deletion in mice and characterization in trabecular meshwork. *Invest Ophthalmol Vis Sci*. 2011;52:2187–2193.
26. Ueda J, Wentz-Hunter K, Yue BY. Distribution of myocilin and extracellular matrix components in the juxtacanalicular tissue of human eyes. *Invest Ophthalmol Vis Sci*. 2002;43:1068–1076.
27. Keller KE, Bradley JM, Vranka JA, Acott TS. Segmental versican expression in the trabecular meshwork and involvement in outflow facility. *Invest Ophthalmol Vis Sci*. 2011;52:5049–5057.
28. Lu Z, Overby DR, Scott PA, Freddo TF, Gong H. The mechanism of increasing outflow facility by rho-kinase inhibition with Y-27632 in bovine eyes. *Exp Eye Res*. 2008;86:271–281.
29. Keller KE, Sun YY, Vranka JA, Hayashi L, Acott TS. Inhibition of hyaluronan synthesis reduces versican and fibronectin levels in trabecular meshwork cells. *PLoS One*. 2012;7:e48523.
30. Zinchuk V, Wu Y, Grossenbacher-Zinchuk O. Bridging the gap between qualitative and quantitative colocalization results in fluorescence microscopy studies. *Sci Rep*. 2013;3:1365.
31. Stamer WD, Seftor RE, Williams SK, Samaha HA, Snyder RW. Isolation and culture of human trabecular meshwork cells by

Investigative Ophthalmology & Visual Science

extracellular matrix digestion. *Curr Eye Res*. 1995;14:611–617.

32. Polansky JR, Weinreb RN, Baxter JD, Alvarado J. Human trabecular cells. I. Establishment in tissue culture and growth characteristics. *Invest Ophthalmol Vis Sci*. 1979;18:1043–1049.
33. Acott TS, Kingsley PD, Samples JR, Van Buskirk EM. Human trabecular meshwork organ culture: morphology and glycosaminoglycan synthesis. *Invest Ophthalmol Vis Sci*. 1988;29:90–100.
34. Keller KE, Bradley JM, Kelley MJ, Acott TS. Effects of modifiers of glycosaminoglycan biosynthesis on outflow facility in perfusion culture. *Invest Ophthalmol Vis Sci*. 2008;49:2495–2505.
35. Pasutto F, Keller KE, Weisschuh N, et al. Variants in ASB10 are associated with open-angle glaucoma. *Hum Mol Genet*. 2012;21:1336–1349.
36. Keller KE, Sun YY, Yang YF, Bradley JM, Acott TS. Perturbation of hyaluronan synthesis in the trabecular meshwork and the effects on outflow facility. *Invest Ophthalmol Vis Sci*. 2012;53:4616–4625.
37. Keller KE, Bradley JM, Acott TS. Differential effects of ADAMTS-1, -4, and -5 in the trabecular meshwork. *Invest Ophthalmol Vis Sci*. 2009;50:5769–5777.
38. Forsberg E, Hirsch E, Frohlich L, et al. Skin wounds and severed nerves heal normally in mice lacking tenascin-C. *Proc Natl Acad Sci U S A*. 1996;93:6594–6599.
39. Mao JR, Taylor G, Dean WB, et al. Tenascin-X deficiency mimics Ehlers-Danlos syndrome in mice through alteration of collagen deposition. *Nat Genet*. 2002;30:421–425.
40. Wang WH, Millar JC, Pang IH, Wax MB, Clark AF. Noninvasive measurement of rodent intraocular pressure with a rebound tonometer. *Invest Ophthalmol Vis Sci*. 2005;46:4617–4621.
41. Saeki T, Aihara M, Ohashi M, Araie M. The efficacy of TonoLab in detecting physiological and pharmacological changes of mouse intraocular pressure–comparison with TonoPen and microneedle manometery. *Curr Eye Res*. 2008;33:247–252.
42. Savinova OV, Sugiyama F, Martin JE, et al. Intraocular pressure in genetically distinct mice: an update and strain survey. *BMC Genet*. 2001;2:12.
43. Aihara M, Lindsey JD, Weinreb RN. Twenty-four-hour pattern of mouse intraocular pressure. *Exp Eye Res*. 2003;77:681–686.
44. Brandt JD. Corneal thickness in glaucoma screening, diagnosis, and management. *Curr Opin Ophthalmol*. 2004;15:85–89.
45. Quackenbush J. Microarray data normalization and transformation. *Nat Genet*. 2002;32(suppl):496–501.
46. Zinchuk V, Zinchuk O, Okada T. Quantitative colocalization analysis of multicolor confocal immunofluorescence microscopy images: pushing pixels to explore biological phenomena. *Acta Histochem Cytochem*. 2007;40:101–111.
47. Rhee DJ, Fariss RN, Brekken R, Sage EH, Russell P. The matricellular protein SPARC is expressed in human trabecular meshwork. *Exp Eye Res*. 2003;77:601–607.
48. Hann CR, Fautsch MP. The elastin fiber system between and adjacent to collector channels in the human juxtacanalicular tissue. *Invest Ophthalmol Vis Sci*. 2011;52:45–50.
49. Santas AJ, Bahler C, Peterson JA, et al. Effect of heparin II domain of fibronectin on aqueous outflow in cultured anterior segments of human eyes. *Invest Ophthalmol Vis Sci*. 2003;44:4796–4804.
50. Gonzalez JM Jr, Hu Y, Gabelt BT, Kaufman PL, Peters DM. Identification of the active site in the heparin II domain of fibronectin that increases outflow facility in cultured monkey anterior segments. *Invest Ophthalmol Vis Sci*. 2009;50:235–241.
51. Midwood KS, Schwarzbauer JE. Tenascin-C modulates matrix contraction via focal adhesion kinase- and Rho-mediated signaling pathways. *Mol Biol Cell*. 2002;13:3601–3613.
52. Midwood KS, Orend G. The role of tenascin-C in tissue injury and tumorigenesis. *J Cell Commun Signal*. 2009;3:287–310.
53. To WS, Midwood KS. Cryptic domains of tenascin-C differentially control fibronectin fibrillogenesis. *Matrix Biol*. 2010;29:573–585.
54. Chiquet-Ehrismann R, Kalla P, Pearson CA, Beck K, Chiquet M. Tenascin interferes with fibronectin action. *Cell*. 1988;53:383–390.
55. Bornstein P, Sage EH. Matricellular proteins: extracellular modulators of cell function. *Curr Opin Cell Biol*. 2002;14:608–616.
56. Bradley JM, Vranka J, Colvis CM, et al. Effect of matrix metalloproteinases activity on outflow in perfused human organ culture. *Invest Ophthalmol Vis Sci*. 1998;39:2649–2658.
57. Bradshaw AD. The role of SPARC in extracellular matrix assembly. *J Cell Commun Signal*. 2009;3:239–246.
58. Oh DJ, Kang MH, Ooi YH, Choi KR, Sage EH, Rhee DJ. Overexpression of SPARC in human trabecular meshwork increases intraocular pressure and alters extracellular matrix. *Invest Ophthalmol Vis Sci*. 2013;54:3309–3319.

Investigative Ophthalmology & Visual Science